Available online at www.sciencedirect.com
SCIENCE DIRECT
Journal of Molecular Catalysis A: Chemical 245 (2006) 69–77
JOURNAL OF MOLECULAR CATALYSIS A: CHEMICAL
www.elsevier.com/locate/molcata

Liquid phase condensation of anisole with *p*-formaldehyde over benzylsulfonic acid functionalized mesoporous Zr-TMS catalysts

M. Chidambaram, S. Selvakumar, T. Tamil Selvi, A.P. Singh *

Catalysis Division, National Chemical Laboratory, Pune 411008, India

Received 28 July 2005; received in revised form 16 September 2005; accepted 23 September 2005
Available online 4 November 2005

Abstract

The catalytic liquid phase condensation of anisole to 4,4′-dimethoxydiphenylmethane (4,4′-DMDPM) with *para*-formaldehyde (*p*-HCHO) has been studied in a batch reactor at atmospheric pressure using of different loadings of benzylsulfonic acid (BSA) functionalized mesoporous Zr-TMS (Zr-TMS-BSA/(–Zr–O–CH_2–Φ–SO_3H)) catalysts. Conventional catalyst, *p*-toluene sulfonic acid (*p*-TSA) and sulfated zirconia and Zr-TMS (zirconia-based transition metal oxide mesoporous molecular sieves) are also included for comparison. Under identical reaction conditions, Zr-TMS-BSA is considerably more active than Zr-TMS and less active than sulfated zirconia and *p*-TSA, however, Zr-TMS-BSA showed higher selectivity among all catalysts. The conversion of anisole, rate of anisole conversion (TOF), selectivity to 4,4′-DMDPM and 4,4′-/2,2′-DMDPM ratio over Zr-TMS-BSA-10, after 6 h of reaction time at 100 °C are ca. 28.2 wt.%, 12.04 h^{-1} mol^{-1} S, 78.5 wt.% and 27.55, respectively. Acidity and mesoporosity of the Zr-TMS-BSA catalyst play important role in the conversion of anisole, rate of anisole conversion and product distribution. The effect of various parameters such as duration of run, reaction time, catalyst concentration, reaction temperature, anisole/*p*-CHCO molar ratio and reuse of catalyst, on the catalyst performance are examined in order to optimize the conversion of anisole and selectivity to 4,4′-DMDPM. The conversion of anisole using Zr-TMS-BSA-10 is increased significantly with the increases in reaction time, catalyst concentration, reaction temperature and decreased with the increase of anisole/*p*-HCHO molar ratio. Zr-TMS-BSA-10 catalyst is recycled two times and a decrease in anisole conversion is observed after second cycle, which is related to the minor leaching of anchored benzylsulfonic acid.

Keywords: Zr-TMS-BSA; Benzylsulfonic acid; Condensation of anisole; *p*-formaldehyde; 4,4′-dimethoxydiphenylmethane

1. Introduction

Derivatives of 4,4′-dimethoxydiphenylmethane (4,4′-DMDPM) is used mainly in polymer industry to manufacture polymer products [1–3]. Bisphenol derivative of 4,4′-DMDPM were reported to polymerize through peroxidase catalysis to give soluble polymers despite bifunctional monomers [4]. It is being used in the development of electronic components, particularly electronic indicating devices, characterized inter alia, by a flat structure and richness in image contrast, compared, for example, to conventional counter or cathode-ray tubes; liquid crystals with a nematic phase have served for several years as picture screen material [5]. Photoinduced electron transfer of 4,4′-DMDPM with any compound like quinines, chloranil forms radical ions and the activity of the two radical ions is of great interest because these intermediates are involved in photoinduced processes of biological (photosynthesis and respiration) and industrial interest [6–9]. Disubstituted diphenylmethanes are also used as intermediates for pharmaceutical and agricultural chemicals [10]. Hydroxylation of 4,4′-DMDPM gives bisphenol-F, which is most wanted product in polymer and pharmaceutical industry. It gives high whiteness background and high d. images showing good resistance to plasticizers [11]. Also, derivatives of 4,4′-DMDPM is extensively used in canned foods as additives [12]. Bisphenol-F, a derivative of 4,4′-DMDPM is a starting material used in the manufacture of most types of epoxy resins, which are then cross-linked and used to coat food cans. *p*-Toluene sulfonic acid (*p*-TSA) is widely used in many condensation reactions [13–18]. However, the recovery of the *p*-TSA from the reaction mixture results in the formation of large amounts of waste, which is environmentally unacceptable. Moreover, the above used catalyst has several disadvantages; wasting a lot of homogeneous catalyst, because the reaction being mainly equimolar and of the difficulty of recycling it after

* Corresponding author. Tel.: +91 20 2590 2497; fax: +91 20 2589 3761.
E-mail address: ap.singh@ncl.res.in (A.P. Singh).

1381-1169/$ – see front matter © 2005 Elsevier B.V. All rights reserved.
doi:10.1016/j.molcata.2005.09.033

use, and corrosion of containers by evolved acidic gases [19]. In order to overcome these difficulties, solid acid catalyst such as Nafion-H, clay, heteropoly acids, metal oxides promoted by sulfate ions (SO_4^{2-}/Al_2O_3, SO_4^{2-}/ZrO_2, SO_4^{2-}/TiO_2, $FeSO_4$ and $Fe_2(SO_4)_3$, SO_4^{2-}/SnO_2, SO_4^{2-}/Al_2O_3, SO_4^{2-}/HfO_2, SO_4^{2-}/Fe_2O_3) have been used. But these catalysts have non-shape selective nature and insufficient acidity in some cases. Zirconium oxide is of particular interest because it contains both acidic and basic surface sites. Also, zirconia has a high melting point, low thermal conductivity, high corrosion resistance, and amphoteric behavior, all of which can be useful properties for a support material. The possibility of obtaining such materials with a mesoporous texture has made this oxide even more interesting [20]. The desire to perform acid-catalyzed reactions over solids has resulted in new research in this area and supported sulfonic acid is now becoming available to replace homogeneous acid solutions [21–23]. Hence, the benzylsulfonic acid functionalized Zr-TMS (Zr-TMS-BSA) catalyst [24] was chosen to meet all the requirements for acid-catalyzed reactions. In this paper we disclose the report of our studies on the catalytic activity of an environmentally friendly, acidic, stable and recyclable Zr-TMS-BSA catalyst in the liquid phase condensation of anisole with *p*-HCHO at atmospheric pressure. Herein, we also report the influence of different wt.% loading of benzylsulfonic acid on Zr-TMS, duration of run, reaction time, catalyst concentration, reaction temperature, molar ratios of reactants and reuse of the catalyst (Zr-TMS-BSA-10) on the conversion of anisole and selectivity to 4,4′-DMDPM. The results obtained over benzylsulfonic acid functionalized mesoporous Zr-TMS catalyst are compared with *p*-TSA, sulfated zirconia and Zr-TMS.

2. Experimental

2.1. Synthesis of Zr-TMS

The Zr-TMS was synthesized by adopting the following molar composition, $0.1Zr(OC_4H_9)_4$:1.4BuOH:0.025CTMABr: 0.03TMAOH:$4H_2O$:0.05Acac:0.5EtOH.

Mesoporous zirconium hydroxide (Zr-TMS) was synthesized by sol–gel route using zirconium butoxide (80 wt.% solution in 1-butanol, Aldrich, USA) as the zirconia source and *N*-cetyl-*N*,*N*,*N*-trimethyl ammonium bromide (CTMABr, S.D. Fine-Chem. Ltd., India) as surfactant at a pH of 11.5, which was maintained by tetramethyl ammonium hydroxide (TMAOH 25 wt.% aq. solution, S.D. Fine-Chem. Ltd., India) solution. Acetyl acetone (Acac) and ethanol controlled the rate of hydrolysis of zirconium butoxide in water. In a mixture of water (4 mol) and TMAOH (0.03 mol), CTMABr (0.025 mol) was dissolved and stirred for 1 h. Then a mixture of zirconium butoxide (0.1 mol), acetyl acetone (0.05 mol) and ethanol (0.5 mol) were added to the template solution slowly and allowed to stir for 3 h. Further, the mixture was refluxed under stirring for 48 h at 90 °C. The resulting solid was filtered, washed with acetone and dried for 10 h at 100 °C (Step 1 of Scheme 1).

2.2. Synthesis of functionalized mesoporous Zr-TMS (Zr-TMS-BSA)

In the first step, the functionalization of benzyl alcohol (0.1 mol, Merck) over Zr-TMS was carried out by etherification reaction using cyclohexane (0.35 mol, Thomas Baker, India) as solvent at 80 °C for 10 h (Step 2 of Scheme 1). The sample was filtered and washed with cyclohexane, benzene and finally with acetone and dried for 6 h at 50 °C. To protect the unloaded hydroxyl groups, after modification with benzyl alcohol, desired amount of Zr-TMS-B was degassed at 80 °C for 2 h and dry toluene was added. Then an excess of ethoxytrimethylsilane was added and the suspension was refluxed at 70 °C under nitrogen atmosphere for 12 h (Step 3 of Scheme 1). The solid was filtered and soxhlet extraction was done with dichloromethane for 12 h and dried at 50 °C for 5 h. Further, sulfonation of the resulting material, Zr-TMS-BS was done with the appropriate amount of chlorosulfonic acid (Spectrochem, India) using chloroform (0.12 mol, Merck India) as solvent at 70 °C for 3 h (Step 4 of Scheme 1). The chlorosulfonic acid was added slowly by a syringe to the mixture of Zr-TMS-BS and chloroform. Thus the material obtained was washed with chloroform and soxhlet extraction was done with a mixture of 1:1 diethyl ether and dichloromethane and dried at 50 °C for 6 h. Benzyl alcohol and sulfonic acid functionalized Zr-TMS are designated as, Zr-TMS-B and Zr-TMS-BSA, respectively.

SO_4^{2-}/ZrO_2 was obtained from MEL Chemicals, Manchester, UK and activated at 500 °C for 10 h under static air prior to reaction.

2.3. Catalyst characterization

The powder X-ray diffraction patterns of synthesized Zr-TMS and Zr-TMS-BSA were recorded on a Rigaku Miniflex (Ni-filtered Cu Kα radiation, λ = 1.5404 Å). The BET surface area, total pore volume, and average pore diameter were measured by N_2 adsorption–desorption method by NOVA 1200 (Quantachrome) at −196 °C. For this particular measurement, the samples were activated at 100 °C for 3 h under vacuum and then the adsorption–desorption was conducted by passing nitrogen onto the sample, which was kept under liquid nitrogen. The FT-IR spectra were obtained in a range 400–4000 cm^{-1} on a Shimadzu FTIR 8201 PC using a Diffuse Reflectance scanning disc technique. Elemental analysis for C and S were done by EA1108 Elemental Analyzer (Carlo Erba Instruments). Temperature-programmed desorption (TPD) measurements were carried out to measure the acid strength of Zr-TMS-BSA with various loading of benzylsulfonic acid, and Zr-TMS using ammonia as an adsorbate [25–27]. In a typical run, 1.0 g of activated sample was placed in a silica tubular reactor and heated at 200 °C under nitrogen flow of 50 ml/min for 6 h. The reactor was then cooled at 30 °C and adsorption conducted at that temperature by exposing the sample to ammonia (10 ml/min) for 30 min. Physically adsorbed ammonia was removed by purging the sample with a nitrogen stream flowing at 50 ml/min for 15 h at 30 °C. The acid strength distribution was obtained by raising the catalyst temperature (10 K/min) from 30 to 200 °C in a number of steps with

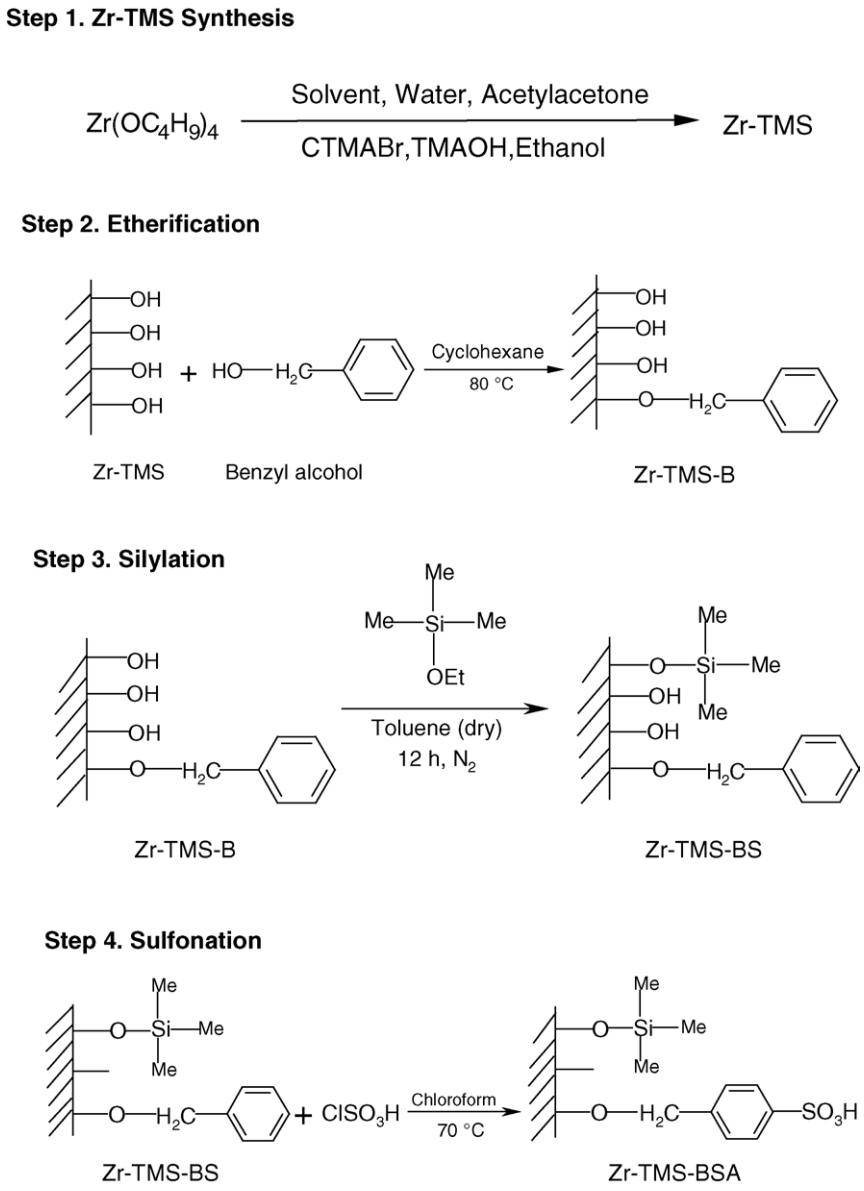

Scheme 1. Synthesis of Zr-TMS and functionalization of benzylsulfonic acid over Zr-TMS. Step 1: Zr-TMS synthesis; Step 2: etherification of Zr-TMS with benzyl alcohol; Step 3: silylation of Zr-TMS-B; Step 4: sulfonation of Zr-TMS-BS.

the flow of nitrogen (50 ml/min). The NH_3 evolved was trapped in the HCl solution and titrated with a standard NaOH solution.

2.4. Condensation of anisole

High purity anisole and A.R. grade *p*-HCHO were used without further purification. The catalyst was activated at 100 °C for at least 4 h before use in the experiments, so as to maintain the dry conditions. The liquid phase catalytic condensation (Scheme 2) was performed in a 50 ml round bottom flask fitted with a condenser, N_2 gas supply tube and a septum. The temperature of the reaction vessel was maintained using an oil bath. In a typical run, a mixture of anisole (0.02 mol), *p*-HCHO (0.01 mol) and activated catalyst (0.1 gm), was magnetically stirred and heated to attain the reaction temperature (100 °C). The product samples were withdrawn at regular intervals of time and analyzed periodically on a gas chromatograph (Agilent 6890N) equipped with a flame ionization detector and a capillary column (5 μm thick cross-linked methyl silicone gum, 0.2 mm × 50 m long). The product samples were also identified by GCMS (Shimadzu 2000 A) analysis. The geometry optimization of diphenyl ether has been done by performing a restricted Hartree-Fock (RHF) calculation using a STO-3G basis set. The calculations are done in Gamess US ab initio quantum chemistry package. The main product, 4,4′-dimethoxydiphenylmethane is separated by column chromatography and confirmed by ^{1}H and ^{13}C NMR analysis.

Conversion of anisole is defined as the weight percentage of anisole consumed. The turnover rates for anisole conversion (TOF, $h^{-1}\,mol^{-1}\,S$) were calculated as the moles of anisole converted per hour over per mol of sulfur. The selectivity to a product is expressed as the amount of a particular product

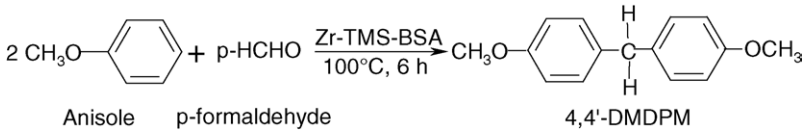

Scheme 2. Liquid phase condensation of anisole with *p*-formaldehyde to 4,4′-dimethoxydiphenlymethane.

divided by the amount of total products and multiplied by 100.

2.5. Identification of main product (4,4′-dimethoxydiphenylmethane)

The main product of our interest, 4,4′-dimethoxydiphenylmethane has been identified by GC, GC–MS, ^{1}H and ^{13}C liquid state nuclear magnetic resonance techniques. GC gave three disguisable product peaks with one prominent peak. The GC–MS gave the molecular weight of dimethoxydiphenylmethane. Further, the main product (4,4′-DMDPM) has been separated by column chromatography and analyzed by ^{1}H and ^{13}C NMR. ^{13}C NMR ($CDCl_3$, adamantane) δ 40.08 (–CH_2), 55.18 (–OCH_3), 133.68 (1), 157.89 (4), 113.82 (2, 6), 129.68 (3, 5). ^{1}H NMR ($CDCl_3$, TMS) δ 3.78 (S, 6H), 3.87 (S, 2H), 6.83 (D, J = 8 Hz, 2H), 7.10 (D, J = 8 Hz, 2H).

3. Results and discussion

3.1. Catalyst characterization

The physico-chemical properties of various catalysts used in this study are presented in Table 1, which lists the elemental analysis highlighting the output of carbon and sulfur (wt.%), loading of benzylsulfonic acid (wt.%), BET surface area, pore diameter and pore volume. These data reveal that Zr-TMS-BSA catalysts are highly mesoporous. Table 1 also illustrates the amount of NH_3 desorbed from various catalysts in different temperature steps, which shows the acidic nature of the catalyst. The detailed characterizations of the catalyst have been reported in our previous report [24].

3.2. Nitrogen sorption study

The surface area, total pore volume and average pore diameter of the Zr-TMS, B-Zr-TMS and BSA-Zr-TMS-10 were found to be 370 $m^2\,g^{-1}$, 0.31 $cm^3\,g^{-1}$, 30.9 Å; 308 $cm^2\,g^{-1}$, 0.28 $cm^3\,g^{-1}$, 26.4 Å and 198 $m^2\,g^{-1}$, 0.18 $cm^3\,g^{-1}$, 18.2 Å, respectively (Table 1). These results demonstrate that the surface area, pore volume and pore diameter of the functionalized materials decrease due to the anchoring of benzyl group over Zr-TMS and further functionalization of B-Zr-TMS with $ClSO_3H$. The surface area, pore volume and average pore diameter of SO_4^{2-}/ZrO_2 are found to be 101 $m^2\,g^{-1}$, 0.09 $cm^3\,g^{-1}$ and 9 Å (Table 1), respectively.

3.3. Acidity of various catalysts

In order to gain an understanding of the acidity of the catalyst, the desorption of NH_3 was carried out in four steps (30–70, 70–110, 110–150, and 150–200 °C) after allowing the catalyst to adsorb ammonia at room temperature and flushed with nitrogen to remove physisorbed ammonia. Table 1 also shows the total number of acid sites (determined via NH_3 chemisorbed at 30 °C) of Zr-TMS, Zr-TMS-BSA-5, -10, -15. The quantitative distributions of the acid sites (in four regions) are also shown. The total number of acid sites on the catalysts was found to increase proportionally with increased loading of benzylsulfonic acid over Zr-TMS. The total number of acid sites on the Zr-TMS was found to be 0.50 mmol g^{-1}. The total amount of NH_3 chemisorbed at 30 °C was 0.72 mmol g^{-1} for Zr-TMS-BSA-5, 1.19 mmol g^{-1} for Zr-TMS-BSA-10 and 1.22 mmol g^{-1} for Zr-TMS-BSA-15 (Fig. 1). The total acidity (desorbed from 30 to 500 °C) of sulfated zirconia is found to be 1.45 mmol g^{-1}.

Table 1
Physico-chemical properties of different catalysts

Catalyst	Elemental analysis (output)[a] (wt.%)		Loading of sulfonic acid (wt.%)		BET surface area ($m^2\,g^{-1}$)[b]	NH_3 desorbed (mmol g^{-1})				NH_3 chemisorbed at 30 °C (mmol g^{-1})[c]
	C	S	Input	Output		30–70 °C	70–110 °C	110–150 °C	150–200 °C	
Zr-TMS[d]					370	0.06	0.15	0.19	0.10	0.50
BSA-Zr-TMS-5[e]	2.9	2.0	5	4.7	229	0.11	0.26	0.31	0.04	0.72
BSA-Zr-TMS-10[f]	1.6	2.5	10	9.1	198	0.23	0.38	0.41	0.17	1.19
BSA-Zr-TMS-15	1.1	2.8	15	10.3	179	0.22	0.39	0.43	0.18	1.22
SO_4^{2-}/ZrO_2[g]	–	2.6	10	7.9	101	–	–	–	–	1.45[h]

[a] Measured by EA1108 CHN/S Elemental Analyzer to measure the acid loading.
[b] Measured by N_2 adsorption–desorption at −196 °C.
[c] Total acid sites determined in the solid catalyst by NH_3 adsorption–desorption from 30 to 200 °C.
[d] Total pore volume is 0.31 $cm^3\,g^{-1}$, average pore diameter is 30.9 Å for Zr-TMS.
[e] Numbers denote wt.% (input) of sulfonic acid loading over Zr-TMS-B.
[f] Total pore volume is 0.18 $cm^3\,g^{-1}$, average pore diameter is 18.2 Å for Zr-TMS-BSA-10.
[g] Total pore volume is 0.09 $cm^3\,g^{-1}$, average pore diameter is 9 Å for SO_4^{2-}/ZrO_2.
[h] Ammonia desorbed from 30 to 500 °C in six steps.

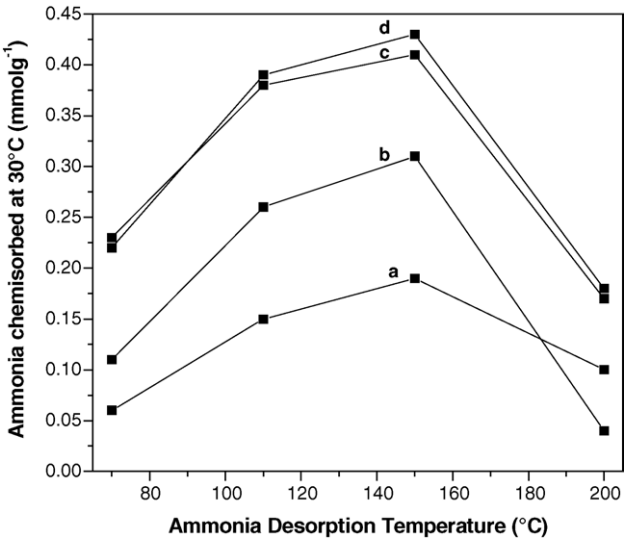

Fig. 1. Ammonia TPD profile for evaluation of acidity for (a) Zr-TMS, (b) Zr-TMS-BSA-5, (c) Zr-TMS-BSA-10 and Zr-TMS-BSA-15 catalysts.

3.4. Catalytic activity of various catalysts

The results of the catalytic activities in the condensation of anisole with *p*-HCHO using conventional catalyst *p*-TSA, commercial ZrO_2/SO_4^{2-}, synthesized Zr-TMS and various amounts of benzylsulfonic acid anchored over Zr-TMS (Zr-TMS-BSA) catalysts are depicted in Table 2. The main product of the reaction is 4,4′-DMDPM. A considerable amount of 2,4′-DMDPM and a small amount of 2,2′-DMDPM are also observed over Zr-TMS and Zr-TMS-BSA catalysts. But with sulfated zirconia and *p*-TSA, considerable amount of other products are also observed which were not identified and may be polymerized products which are formed due to their strong acidic nature. The formation of DMDPM results from the aromatic substitution of anisole. The activities of various catalysts are compared under identical reaction conditions using data after 6 h run.

The conversion of anisole, rate of anisole conversion, product distribution and ratio of 4,4′-DMDPM to 2,2′-DMDPM depend on the type of catalysts used. As can be seen from Table 2, Zr-TMS-BSA-15 catalyst is found to be more active than any other catalysts. Zr-TMS is less active due to its lower acidic nature. The conversion of anisole, rate of anisole conversion, selectivity for 4,4′-DMDPM and 4,4′-DMDPM/2,2′-DMDPM ratio over Zr-TMS-BSA-5, Zr-TMS-BSA-10, Zr-TMS-BSA-15 and Zr-TMS after 6 h of reaction time are found to be 12.6, 28.2, 43.9, 2.0 wt.%; 6.7, 12.0, 16.7 h^{-1} mol^{-1} S; 75.1, 78.6, 78.2, 82.0 wt.% and 20.3, 28.1, 29.2, 27.3, respectively. *p*-TSA and sulfated zirconia produce 35.4, 61.1 wt.% (conversion of anisole), 429.4, 25.1 h^{-1} mol^{-1} S (TOF), 69.7, 68.7 wt.% (selectivity for 4,4′-DMDPM), and 9.3, 10.1 (4,4′-DMDPM/2,2′-DMDPM ratio), respectively. Amongst the Zr-TMS-BSA-5, -10, -15, Zr-TMS-BSA-15 revealed the highest anisole conversion and rate of anisole conversion, which may be attributed to its higher acidity as seen from NH_3 desorption experiment (Table 1). The catalysts used in this study, show the following decreasing order of activity after 6 h of reaction time: ZrO_2/SO_4^{2-} > Zr-TMS-BSA-15 > *p*-TSA > Zr-TMS-BSA-10 > Zr-TMS-BSA-5 > Zr-TMS. Whereas the selectivity to 4,4′-DMDPM is in the order of Zr-TMS > Zr-TMS-BSA-10 > Zr-TMS-BSA-15 > Zr-TMS-BSA-5 > *p*-TSA > ZrO_2/SO_4^{2-}. The results indicate that mainly *para*-substitutions take place over Zr-TMS-BSA catalyst. The molecular size of 4,4′-DMDPM, 2,4′-DMDPM and 2,2′-DMDPM were found to be 12.40979, 10.65782 and 9.22677 Å (horizontal), respectively, which clearly show that the diffusion of products from pores of various Zr-TMS catalysts is highly possible and hindered from the pores or the interlayer distance of sulfated zirconia catalyst, which further shows that in sulfated zirconia, catalysis takes place on the surface.

3.5. Influence of reaction time using Zr-TMS-BSA-10

The influence of reaction time on the conversion of anisole, rate of anisole conversion, product distribution and 4,4′-DMDPM/2,2′-DMDPM ratio using Zr-TMS-BSA-10 as catalyst at 100 °C is presented in Fig. 2. The conversion of anisole increased almost linearly up to 12 h of reaction time and then a marginal increase in the conversion of anisole is observed at 24 h of reaction time. The anisole along with *p*-HCHO leads mainly to 4,4′-DMDPM with 79.8 wt.% selectivity within 0.5 h reaction

Table 2
Catalytic activity of various catalysts[a]

Catalysts	Conversion of anisole (wt.%)	TOF[b] (h^{-1} mol^{-1} S)	Product distribution (wt.%)[c]				4,4′-/2,2′-DMDPM ratio[d]
			4,4′-DMDPM	2,4′-DMDPM	2,2′-DMDPM	Others	
Zr-TMS	2.0	–	82.0	15.0	3.0	0.0	27.3
Zr-TMS-BSA-5	12.6	6.7	75.1	21.2	3.7	0.0	20.3
Zr-TMS-BSA-10	28.2	12.0	78.6	18.6	2.8	0.0	28.1
Zr-TMS-BSA-15	43.9	16.7	78.2	19.1	2.7	0.0	29.2
p-TSA[e]	35.4	429.4	69.7	14.7	7.5	8.1	9.3
SO_4^{2-}/ZrO_2	61.1	25.1	68.7	19.8	6.8	4.7	10.1

[a] Reaction conditions: catalyst (g) = 0.1; anisole (mmol) = 20; *p*-HCHO (mmol) = 10; reaction temperature (°C) = 100; reaction time (h) = 6.
[b] TOF = moles of anisole transformed per hour per mole of sulfur.
[c] 4,4′-DMDPM = 4,4′-dimethoxydiphenylmethane; 2,4′-DMDPM = 2,4′-dimethoxydiphenylmethane; 2,2′-DMDPM = 2,2′-dimethoxydiphenylmethane.
[d] Ratio of 4,4′-dimethoxydiphenylmethane/2,2′-dimethoxydiphenylmethane.
[e] Amount of catalyst used (g) = 0.01.

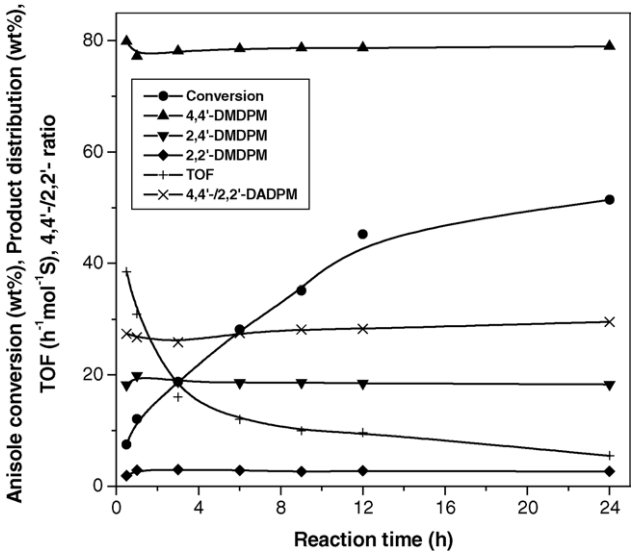

Fig. 2. Conversion of anisole (wt %) vs. reaction time over Zr-TMS-BSA-10 catalysts. Reaction conditions: catalyst (g) = 0.1; anisole (mmol) = 20; *p*-HCHO (mmol) = 10; reaction temperature (°C) = 100; reaction time (h) = 6.

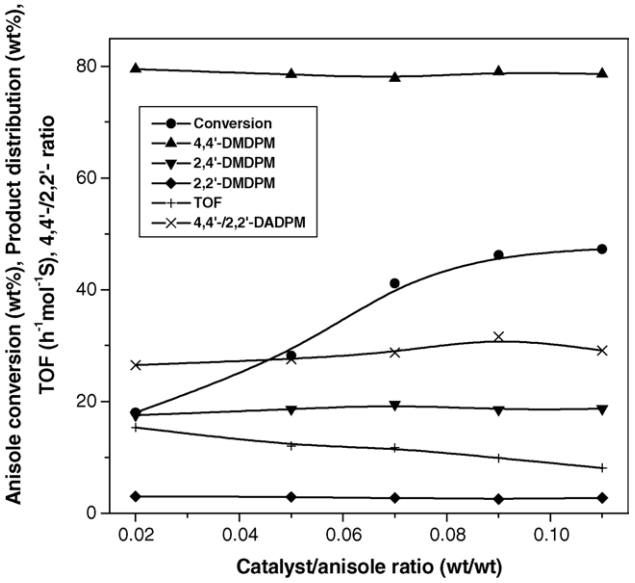

Fig. 3. Effect of catalyst/anisole (w/w) ratio on the conversion of anisole (wt.%), product distribution (wt.%), TOF (h^{-1} mol^{-1} S) and 4,4′-DMDPM/2,2′-DMDPM isomer ratio. Reaction conditions: catalyst (g) = 0.05, 0.1, 0.15, 0.2 and 0.25; anisole (mmol) = 20; *p*-HCHO (mmol) = 10; reaction temperature (°C) = 100; reaction time (h) = 6.

time and ended with 79.0 wt.% after 24 h. The anisole conversion, rate of anisole conversion, selectivity to 4,4′-DMDPM and 4,4′-/2,2′-DMDPM ratio after 24 h or reaction time were found to be 51.4 wt.%, 5.5 h^{-1} mol^{-1} S, 79.0 wt.% and 29.6, respectively. The results show that the reaction time influence the conversion of anisole, but did not affect significantly the 4,4′-DMDPM selectivity and 4,4′-DMDPM/2,2′-DMDPM isomer ratio.

3.6. Influence of catalyst/anisole (w/w) ratio

To study the effects of catalyst concentration on the conversion of anisole, rate of anisole conversion, product distribution and 4,4′-/2,2′-isomer ratio, the catalyst concentration (catalyst/anisole ratio (w/w)) was increased from 0.02 to 0.11 and the results are depicted in Fig. 3. The different ratios of catalyst/anisole were obtained by varying the amount of catalyst and keeping the concentration of anisole constant. The conversion of anisole increased from 18.0 to 47.3 wt.% as the catalyst concentration increases from 0.02 to 0.11. Not much difference in the product distribution is seen against the change in catalyst concentration. The rate of anisole conversion (TOF) decreases continuously due to the increase in catalyst concentration due to the corresponding increase in the concentration of sulfur in the total amount of catalyst used. It may be seen that the catalyst/anisole (w/w) ratio had a strong effect on the conversion of anisole. A rapid increase in the conversion of anisole is observed from 0.02 to 0.07 of the reaction and very slow activity is observed from 0.07 to 0.11 of the catalyst/anisole (w/w) ratios. By using 0.11 ratio of catalyst/anisole, the conversion of anisole, rate of anisole conversion, 4,4′-DMDPM selectivity and 4,4′-/2,2′-DMDPM ratio are found to be 47.3 wt.%, 8.1 h^{-1} mol^{-1} S, 78.6 wt.%, and 29.1, respectively.

3.7. Influence of reaction temperature

The effect of reaction temperature was studied on the rate of condensation of anisole with *p*-formaldehyde over Zr-TMS-BSA-10 catalyst in the temperature range 90–120 °C using an anisole/*p*-HCHO molar ratio as 2 and the reaction time as 6 h (Fig. 4). When the temperature is increased from 90 to 120 °C, both the conversion of anisole and TOF increased from 17.8 to 37.4 wt.% and 7.6 to 16.0 h^{-1} mol^{-1} S, respectively. However, the selectivity for 4,4′-DMDPM remains nearly unchanged with the increase in reaction temperature, as shown in Fig. 4.

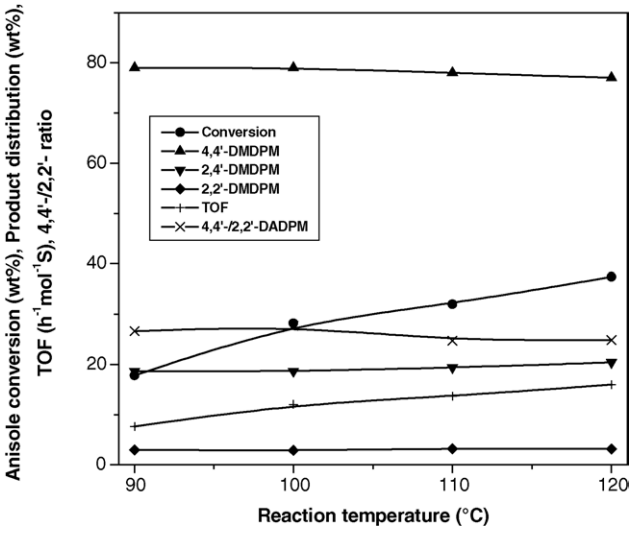

Fig. 4. Effect of different reaction temperatures on the conversion of anisole (wt.%), product distribution (wt.%), TOF (h^{-1} mol^{-1} S) and 4,4′-DMDPM/2,2′-DMDPM isomer ratio. Reaction conditions: catalyst (g) = 0.1; anisole (mmol) = 20; *p*-HCHO (mmol) = 10; reaction temperature (°C) = 90, 100, 110 and 120; reaction time (h) = 6.

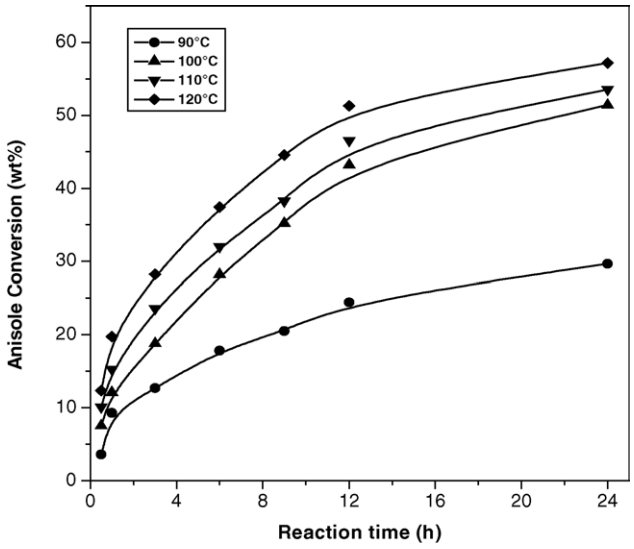

Fig. 5. Effect of reaction temperature (°C) on the conversion of anisole (wt.%) over Zr-TMS-BSA-10 catalyst with respect to reaction time (h). Reaction conditions: catalyst (g) = 0.1; anisole (mmol) = 20; *p*-HCHO (mmol) = 10; reaction temperature (°C) = 90, 100, 110 and 120; reaction time (h) = 6.

One of the reasons for the increased rates at higher temperature may be ascribed to an enhancement of the rate of diffusion of anisole inside the channel of the catalyst; however, reaction rates are usually more temperature dependant than rate of diffusion. The conversion of anisole increases sharply at the initial stages (12 h) of the reaction and finally (24 h) reaches a relatively steady state value over all temperatures as shown in Fig. 5. The apparent activation energy of anisole conversion over Zr-TMS-BSA-10 catalyst is estimated to be 34.03 kJ/mol as it is depicted in Fig. 6 in the temperature range 90–120 °C.

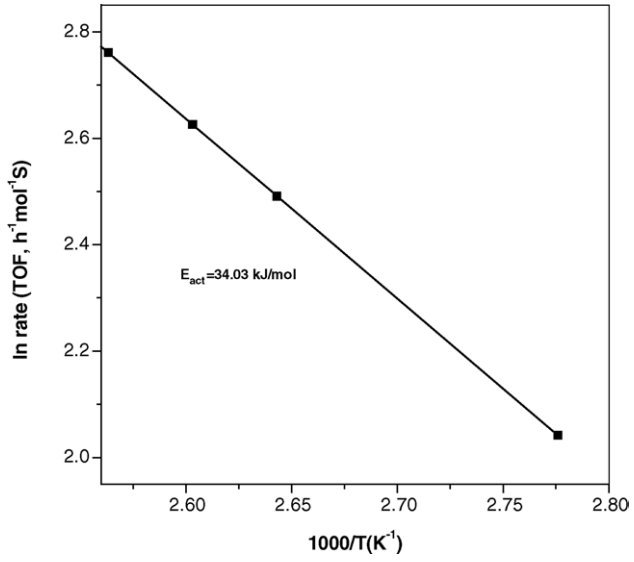

Fig. 6. Arrhenius plot for the condensation of anisole with *p*-HCHO over Zr-TMS-BSA-10; reaction conditions: catalyst (g) = 0.1; anisole (mmol) = 20; *p*-HCHO (mmol) = 10; reaction temperature (°C) = 90, 100, 110 and 120; reaction time (h) = 6.

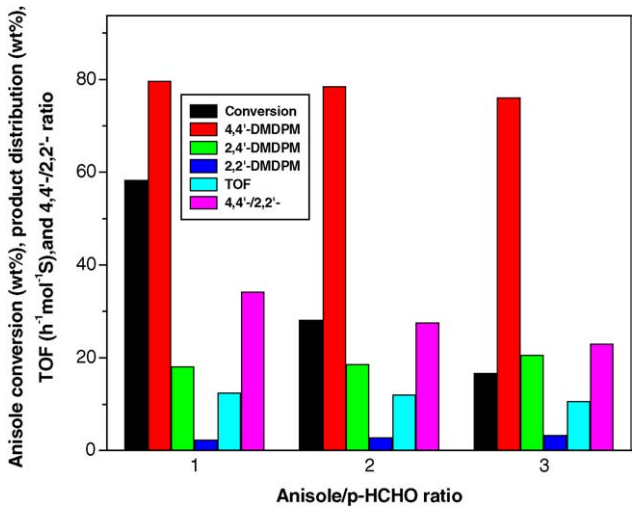

Fig. 7. Effect of anisole/*p*-HCHO molar ratio on the conversion of anisole (wt.%), product distribution (wt.%), TOF (h^{-1} mol^{-1} S) and 4,4′-DMDPM/2,2′-DMDPM isomer ratio. Reaction conditions: catalyst (g) = 0.1; anisole (mmol) = 10, 20, 30; *p*-HCHO (mmol) = 10; reaction temperature (°C) = 100; reaction time (h) = 6.

3.8. Influence of molar ratios of the reactants

The results of the influence of anisole/*p*-HCHO molar ratios on the anisole conversion, TOF, product distribution and 4,4′-DMDPM/2,2′-DMDPM ratio is shown in Fig. 7. The ratios were changed by keeping the amount of anisole as constant. The data show at 100 °C that, when anisole/*p*-HCHO ratio is increased from 1 to 3, the conversion of anisole and rate of anisole conversion decrease linearly from 58.3 to 16.6 wt.% and 12.4 to 10.6 h^{-1} mol^{-1} S, respectively. Since the amount of anisole with respect to *p*-HCHO at the molar ratio of 1:1 (anisole/*p*-HCHO = 1) is less the conversion of anisole is found to be high. In addition, the selectivity to 4,4′-DMDBP is found to be decreased when the molar ratio is increased. Based on the observation, we found that 1:1 molar ratio of anisole:*p*-HCHO is optimum for high conversion of anisole, selectivity to 4,4′-DMDPM and 4,4′-DMDPM/2,2′-DMDPM ratio.

3.9. Comparison of p-HCHO with aq. HCHO as condensation agent

The liquid phase condensation of anisole with formaldehyde was performed using *aqueous*-formaldehyde and *para*-formaldehyde. The 6 h reaction data over these two condensation agents is shown in Fig. 8. As shown in the figure, *aq*-HCHO showed very poor performance than *p*-HCHO. The presence of large quantity of water in the *aq*-HCHO may be deactivating the catalyst and the active species of the catalyst might be leached out from the surface of the support. Though *p*-HCHO is a polymer, it decomposes at about 120 °C and gives monomer, which took part in the catalytic reaction. At 6 h reaction time, the conversion of anisole (wt.%), TOF (h^{-1} mol^{-1} S), selectivity to 4,4′-DMDPM (wt.%) and 4,4′-/2,2′-DMDPM ratio using *aq*-HCHO and *p*-HCHO found to be 3.1, 1.3, 76.5, 22.4 and 28.2, 12.0, 78.5, 27.6, respectively. This experiment clearly shows that

Table 3
Catalyst recycles study[a]

Cycle	Elemental analysis[b] (wt.%)		Conversion of anisole (wt.%)	TOF[c] (h^{-1} mol^{-1} S)	Product distribution (wt.%)[d]			4,4′-/2,2′-DMDPM ratio	Catalyst crystallinity (%)
	C	S			4,4′-DMDPM	2,4′-DMDPM	2,2′-DMDPM		
Fresh	1.6	2.5	28.2	12.0	78.5	18.6	2.9	27.1	100
First recycle	1.3	2.4	25.0	11.1	77.0	19.8	3.2	24.1	99.5
Second recycle	0.9	1.6	15.3	10.2	76.4	20.3	3.3	23.2	89.8

[a] Reaction conditions: catalyst (g) = 0.1; anisole (mmol) = 20; *p*-HCHO (mmol) = 10; reaction time (h) = 6; reaction temperature (°C) = 100.
[b] Elemental analysis by EA1108 Elemental Analyzer (Carlo Erba).
[c] TOF is given as moles of anisole transformed per hour per mole of sulfur.
[d] 4,4′-DMDPM = 4,4′-dimethoxydiphenylmethane; 2,4′-DMDPM = 2,4′-dimethoxydiphenylmethane; 2,2′-DMDPM = 2,2′-dimethoxydiphenylmethane.

p-HCHO is a suitable and far better condensation agent than *aq*-HCHO for this particular reaction.

3.10. Catalyst recycling

In order to check the stability and catalytic activity, the catalyst was recycled (fresh + two cycles) by using Zr-TMS-BSA-10 in the condensation of anisole. The results are presented in Table 3. After workup of the reaction mixture, the catalyst was separated by filtration, washed with water and acetone and activated for 10 h at 100 °C in the presence of air before use in the next experiment. Thus, the recovered catalyst after each reaction was characterized for its chemical composition by elemental analysis and crystallinity by X-ray diffraction (XRD). Elemental analysis showed a downward trend in the content of anchored benzylsulfonic acid of Zr-TMS-BSA-10 catalyst after second cycle. Powder XRD shows the drastic decrease in crystallinity after second recycle (Fig. 9). A slight decline was observed in the anisole conversion from 28.2 to 25 wt.%, and 25 to 15.3 wt.%, when the catalyst was reused for first and second time, respectively. Whereas selectivity to 4,4′-DMDPM decreased from 78.5 to 76.4 wt.%, respectively. The leaching of the benzylsulfonic acid from the Zr-TMS catalysts by water (formed during the reaction) may be attributed for the decrease in catalytic activity after second cycle.

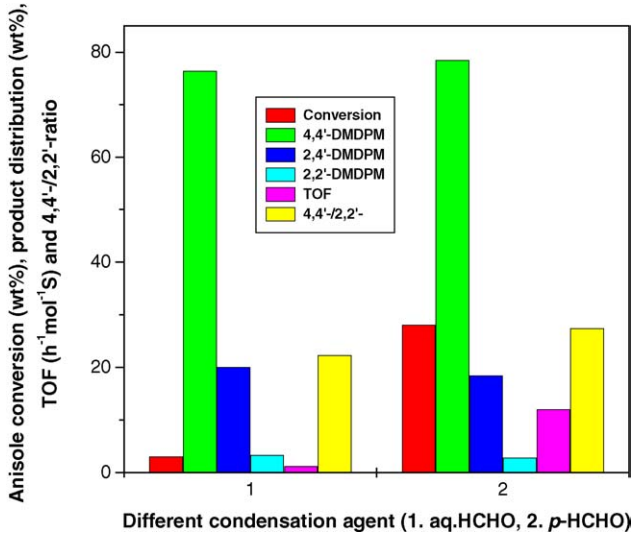

Fig. 8. Effect of different condensation agents on the conversion of anisole (wt.%), product distribution (wt.%), TOF (h^{-1} mol^{-1} S) and 4,4′-DMDPM/2,2′-DMDPM isomer ratio. Reaction conditions: catalyst (g) = 0.1; anisole (mmol) = 20; *p*-HCHO/*aq*-HCHO (mmol) = 10; reaction temperature (°C) = 100; reaction time (h) = 6.

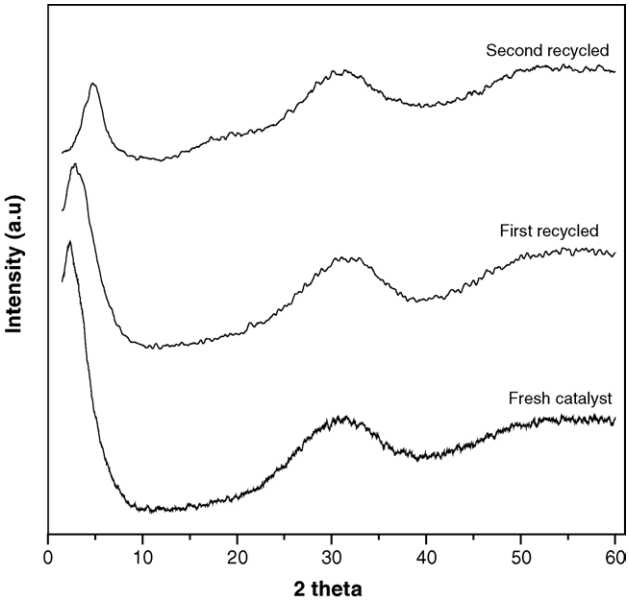

Fig. 9. Powder XRD pattern of fresh, first and second recycled catalysts.

4. Conclusions

In summary condensation of anisole to 4,4′-DMDPM reactions were performed on Zr-TMS-BSA-5, Zr-TMS-BSA-10, Zr-TMS-BSA-15, Zr-TMS, sulfated zirconia and *p*-TSA catalysts. Zr-TMS-BSA-15 catalyst catalyzes the condensation of anisole efficiently with *para*-formaldehyde and is superior to other Zr-TMS-BSA catalysts due to its higher acidity. *p*-TSA, the conventional homogeneous catalyst and sulfated zirconia showed high activity than Zr-TMS and Zr-TMS-BSA catalysts, whereas, Zr-TMS-BSA catalysts were found to be selective than any other studied catalysts. Total acidity obtained at 30 °C of Zr-TMS and Zr-TMS-BSA with different wt.% loading of benzylsulfonic acid show direct co-relationship between acidity and catalytic activity in the condensation of anisole. The influence of the duration of the run, catalyst concentration, reaction temperature and anisole/*p*-HCHO molar ratio on the catalyst

performance is examined in order to optimize the conversion of anisole and selectivity to 4,4′-DMDPM. The conversion of anisole using Zr-TMS-BSA-10 increased significantly with an increase in reaction time, catalyst concentration, and reaction temperature and decreased for anisole to *p*-HCHO molar ratio. Zr-TMS-BSA-10 was recycled two times and a decrease in anisole conversion is observed after two cycles, which is related to a minor leaching of benzylsulfonic acid from the catalyst.

Acknowledgements

MC thanks Council of Scientific and Industrial Research, New Delhi, for Senior Research Fellowship. Authors thank Mr. Akhilesh Tanwar, Theory group of Physical Chemistry division, NCL, for molecular size calculations and CSIR New Delhi-Task Force Project (P23-CMM0005-B) for financial support.

References

[1] H. Uyama, N. Maruichi, H. Tonami, S. Kobayashi, Biomarcomolecules 3 (2000) 187.
[2] S.K. Jana, T. Kugita, S. Namba, Catal. Lett. 90 (2003) 143.
[3] M. Matsura, K. Hirakawa, Japanese Patent JP61204204 (1986).
[4] T. Fukuoka, H. Tonami, N. Maruichi, H. Uyama, S. Kobayashi, H. Higashimura, Macromolecules 33 (2000) 9152.
[5] S. Ralf, US Patent US4002670 (1977).
[6] T.D. Giacco, E. Baciocchi, O. Lanzalunga, F. Elisei, Chem. Eur. J. 7 (2001) 3005.
[7] M.Y. Okamura, G. Feher, Annu. Rev. Biochem. 61 (1992) 861.
[8] A.C. Buchanan, R. Livingston, A.S. Dworkin, G.P. Smith, J. Phys. Chem. 84 (1980) 423.
[9] E. Baciocchi, T.D. Giacco, F. Elisei, O. Lanzalunga, J. Am. Chem. Soc. 120 (1998) 11800.
[10] U. Beck, in: W. Gerhartz, Y.Y. Stephen, F.T. Campbell, R. Pfeffekorn, J.F. Rounsaville (Eds.), Ullmann's Encyclopedia of Industrial Chemistry, vol. A15, VCH, Weinheim, 1986, p. 91.
[11] M. Nakatsuka, Y. Tanabe, K. Yoshikawa, Japan Patent JP08290668 (1996).
[12] A. Goodson, W. Summerfield, I. Cooper, Food Addit. Contam. 19 (2002) 796.
[13] M.P.W. Mahindaratne, K. Wimalasena, J. Org. Chem. 63 (1998) 2858.
[14] M. Oda, T. Noda, European Patent EP812824 (1997).
[15] N. Hoshika, Japan Patent JP10279668 (1998).
[16] R. Kisai, Japan Patent JP2002161058 (2002).
[17] K. Nakahara, M. Kaji, Japan Patent JP2004067569 (2004).
[18] N. Saito, T. Otsuka, K. Fukuda, M. Fujiwara, Japan Patent JP2005097429 (2005).
[19] C. Venkatesan, T. Jaimol, P. Moreau, A. Finiels, A.V. Ramaswamy, A.P. Singh, Catal. Lett. 75 (2001) 119.
[20] V.I. Parvulescu, H. Bonnemann, V. Parvulescu, B. Endruschat, A.Ch.W. Rufinska, B. Tesche, G. Poncelet, Appl. Catal. A 214 (2001) 273.
[21] J.W. Brockington, R.H. Bennett, US Patent US3970721 (1976).
[22] J.F. Joly, C. Marcilly, E. Benazzi, US Patent US5336833 (1994).
[23] S.I. Hommeltoft, European Patent EP0987237A (2000).
[24] S. Parambadath, M. Chidambaram, A.P. Singh, Catal. Today 97 (2004) 233.
[25] N.C. Marziano, L.D. Ronchin, C. Tortato, A. Zingales, A.A. Sheikh-Osman, J. Mol. Catal. A 174 (2001) 265.
[26] M. Chamumi, D. Brunel, F. Fajula, P. Geneste, P. Moreau, J. Solof, Zeolites 14 (1994) 283.
[27] A. Corma, M.I. Fornes, J.M. Juan-Rajadell, L. Neito, Appl. Catal. A 116 (1994) 151.